Stability Analysis of Excavation Fronts at the Herculaneum Archaeological Site

O. Casablanca[1], M. Zimbardo[2], and A. Scotto di Santolo[3]

[1]*Researcher, Pegaso University, Naple, Italy, email: orazio.casablanca@unipegaso.it*

[2]*Researcher, Pegaso University, Naple, Italy, email: margherita.zimbardo@unipegaso.it*

[3]*Professor, Pegaso University, Naple, Italy, email: anna.scottodisantolo@unipegaso.it*

ABSTRACT

Italian cultural heritage represents an invaluable legacy, widely distributed throughout the national territory and often located in areas with high seismic hazard and in complex geomorphological and environmental contexts. This paper addresses the assessment of the stability, under both static and seismic conditions, of the excavation fronts located within the archaeological site of Herculaneum, Italy. To this end, a two-dimensional finite element numerical modelling was carried out, with the aim of reproducing the current safety conditions and estimating the seismic response of the slopes near the Villa of the Papyri, through nonlinear dynamic analyses using seismic inputs compatible with the design spectrum prescribed by current Italian technical regulation. The results of these analyses allow for a preliminary evaluation of the seismic performance of the excavation fronts, by comparing the seismic-induced displacements with reference threshold values, in order to define potential damage mitigation measures for the archaeological structures.

Keywords: Slope Stability; Finite Element Modelling; Seismic performance

INTRODUCTION

Italy's cultural heritage is an invaluable patrimony, broadly distributed across the national landscape and often located in regions of high seismic hazard and complex geomorphological environments. This paper concerns the assessment of the stability, under both static and seismic loading, of the excavation fronts in an important Italian archaeological site. The work specifically examines the context of the Herculaneum archaeological site. Towards this aim, a numerical finite element model under plane-strain conditions was developed, in order to replicate the current stability condition and to estimate the seismic response of the unsaturated slopes in the vicinity of the Villa of the Papyri. This was carried out by means of non-linear dynamic analyses adopting seismic inputs selected on the basis of the spectrum-compatibility with those required by the current Italian technical code. The results from these analyses allows a preliminary estimation of the seismic performance of the excavated slopes. This estimation will relies on a comparison of the displacements induced by seismic loading with standard limit values, with the final aim of outlining potential measures to mitigate damage to the archaeological structures.

DESCRIPTION OF THE STUDY AREA

The catastrophic A.D. 79 eruption of Mount Vesuvius entombed the ancient settlements of Pompeii, Herculaneum, and Stabiae beneath thick pyroclastic deposits, leading to their exceptional preservation. Located about 7 km from the volcano, Herculaneum and its renowned Villa dei Papiri (*VdP*)—a seaside residence famous for its library of philosophical papyri—were buried under approximately 25 m of volcanic material. Centuries of archaeological work at the site, which began in the 18th century, have intermittently exposed portions of the town and the VdP.

The excavations at the Villa dei Papiri have significantly advanced the understanding of its complex multi-level structure. The work brought to light the western part of the atrium quarter and the southwestern prospect of the underlying *basis villae* (Figure 1a). The atrium sector itself, occupies the prominent main level of the complex and offers a panoramic view of the sea. This level, which includes the central atrium and the two large rooms adjacent to it, exhibits a well-balanced spatial distribution indicative of meticulous pre-construction planning. Within this sector, sixteen rooms and a section of the tripartite seaward portico have been excavated, covering an area of approximately 750 m² (Figure 1b). All rooms feature mosaic decorations. Although the 18th-century Bourbon exploration was destructive, wall segments preserved to a height of about 2.9 m remain valuable for interpreting the original architectural arrangement. However, this early exploration was confined to the main level, due to the presence of compact pyroclastic layers and confirmed by the almost absence of tunnels beneath the pavement. The continuation of modern excavation southward therefore revealed a major new discovery: a monumental complex located about 9 m below the atrium level, projecting toward the sea.
The following excavation uncovered the *basis villae*—the substructure upon which the main level was built. Its facade, exposed for 25 m in length and 4 m in height, suggests an extent equal to the atrium quarter above (fig. 1c).
Furthemore, the excavation has thus clarified a vertical succession of four architectonic levels adapted to the natural slope (fig. 1d):

1. Main Level: Situated at 11 m above the sea level.
2. Second Level: Beginning at 6 m above sea level, defined by the *basis villae* facade.
3. Third Level: Beginning at 2 m above sea level, "lower terrace" structure.
4. Fourth Level: Providing access via a staircase down to the ancient beach and now situated at 4.5 m below the current sea level.

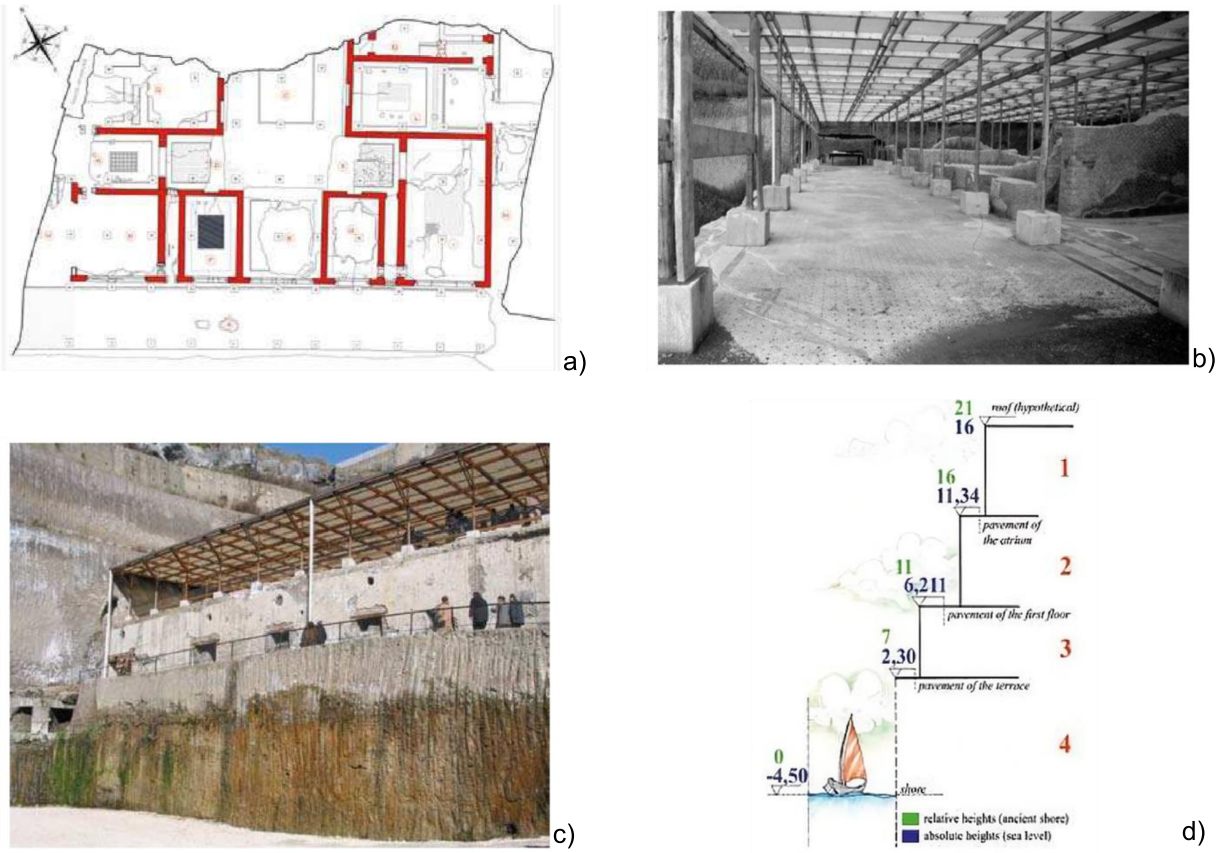

Figure 1. *Villa of the Papyri: a) plan of the atrium quarter and b) view inside portico; c) view of the basis villae and portico of the atrium; d) schematic section of the levels of the Villa of the Papyri (modified after De Simone, 2010).*

The currently excavated area covers approximately 40,000 m², involving the excavation of a deep trench to connect the Herculaneum excavations with the VdP. The excavated trench has resulted in steep artificial slopes approximately 20 m high, due to the implementation of sub-vertical excavations aimed at preserving the buried archeological structures. However, from a geotechnical perspective, such steep slopes may not satisfy the required safety conditions (e.g., Scotto di Santolo et al., 2000). Furthermore, the base of the excavation is situated below sea level, at approximately 4.5 m, requiring a system of pumps to remove infiltrating water (e.g., De Simone, 2010). This dewatering operation directly influences the stability conditions by altering the degree of saturation of the soil within the excavated area. The local stratigraphy comprises a complex sequence of volcanic deposits from multiple eruptions, overlain by a lava flow from the 1631 event. Crucially, the A.D. 79 deposits consist of heterogeneous, weakly cemented tuffaceous ash layers containing pyroclastic fragments. This stratigraphy results in a geotechnical profile where variably saturated, heterogeneous pyroclastic soils overlie more competent tuff bedrock, forming the layered system into which the precarious archaeological slopes have been excavated. Consequently, assessing the stability of these slopes requires a detailed understanding of the mechanical behavior of this specific volcanic sequence, particularly under unsaturated conditions.

NUMERICAL ANALYSES

Numerical model

The numerical analyses were conducted under plane strain conditions, discretizing the soil with a finite element mesh consisting of approximately 5000 15-node triangular elements using the finite element code Plaxis 2D (Bentley, 2022). The model, which includes the various stratigraphic sequences, is presented in Figure 2, along with a plan view showing the trace of the analysis section.

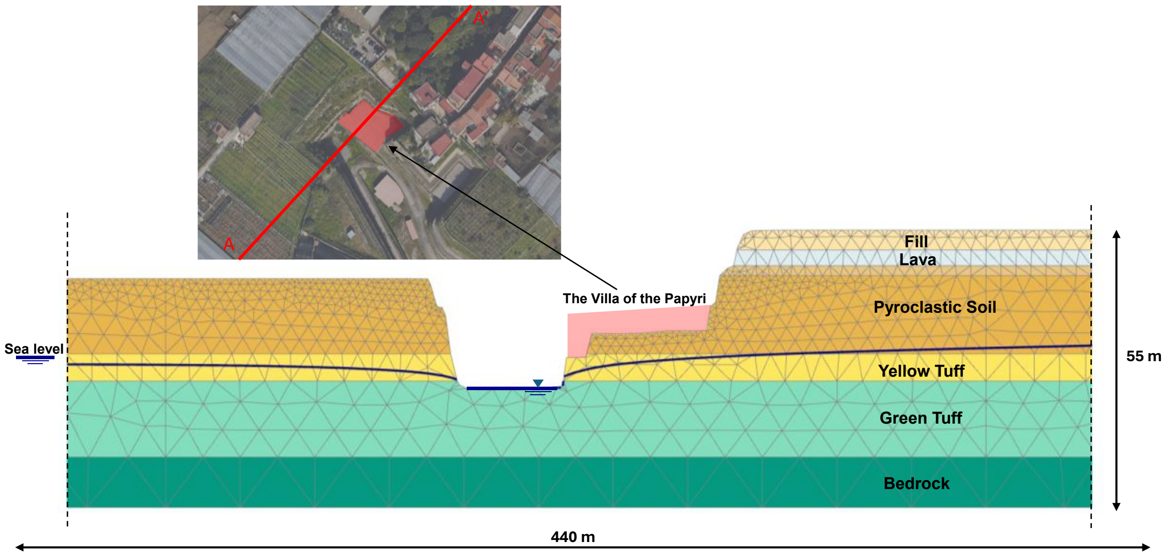

Figure 2. *Finite element mesh used for the analyses and plan view showing the trace of the analysis section.*

In the static analyses, the base nodes were constrained in both directions, while only horizontal displacements were prevented on the vertical boundaries. To account for radiation damping in the dynamic analyses, a compliant bedrock condition was introduced at the base of the mesh, while free-field elements were applied along the vertical sides of the mesh. To avoid numerical distortion of propagating seismic waves, the maximum element height was taken to be less than 1/6 of the wavelength λ_{min} associated with the maximum frequency f_{max} of the input seismic motion. The mesh has a width of 440 m, which is 8 times the model height of 55 m.
The non-linear behaviour of the soil was considered by adopting an elasto-plastic hysteretic model with isotropic hardening, known as the *Hardening Soil model with small-strain stiffness* (Schanz et al., 1999). This model (HSsmall) is capable of describing the non-linear soil behaviour in the small strain range. The parameters of the numerical model were calibrated based on the results of oedometer and drained triaxial compression tests available for the site under investigation. To describe the soil behaviour in the small-strain range, the results of resonant column tests, expressed in terms of normalized shear modulus decay curves (G/G_0) and damping ratio increase (D) as a function of shear strain, performed at confining pressures of 100 kPa on samples of pyroclastics and yellow tuff were used. In the absence of specific cyclic tests for the surface materials (fill and lava) and the green tuff at the base of the

excavation, reference was made to selected data from the literature for defining the input parameters related to these materials. The values of the model parameters associated with the soil layers shown in Figure 2 are summarized in Table 1.

Table 1. *Parameters of the HSsmall model for the soil layers in the study area.*

Soil	γ (kN/m^3)	φ' (°)	c' (kPa)	ψ (°)	E_{50}^{ref} (kPa)	E_{oed}^{ref} (kPa)	E_{ur}^{ref} (kPa)	ν_{ur}	m	G_0^{ref} (kPa)	$\gamma_{0.7}$ (%)
Fill	17.3	30	5	0	64000	64000	240000	0.2	0.7	400000	0.01
Lava	23.7	28	250	0	105000	105000	314900	0.2	0	1312000	0.2
Pyr. Soil	18.6	36	2	0	64000	64000	240000	0.2	1	400000	0.03
Yellow Tuff	14	28	250	0	62500	62500	187600	0.2	0	781600	0.24
Green Tuff	14	28	500	0	92000	92000	276000	0.2	1	1150000	0.24

The bedrock was modelled as a linear elastic material assuming a shear wave velocity Vs = 950 m/s and a unit weight of 14 kN/m^3.
A significant portion of the excavation fronts is in a state of partial saturation; consequently, the assessment of safety conditions requires adequate modeling of the mechanical response of the soils, which depends on the negative pore water pressure (suction) and the degree of saturation.
In this study, the effective stress approach by Bishop, widely validated by numerous experimental and theoretical studies (e.g., Borja et al., 2012), was used to simulate the mechanical behavior of the soils under partially saturated conditions.
The hydraulic behaviour of the soils under partially saturated conditions is expressed by the retention curve, in terms of the relationship between suction and degree of saturation, using the model proposed by Van Genuchten (1980) according to the following Plaxis formulation (Bentley, 2022)

$$S(\phi) = S_{res} + (S_{sat} - S_{res})\left[1 + (g_a|\phi|)^{g_n}\right]^{g_c} \quad (1)$$

where ϕ is the pressure head and g_a, g_n and g_c are model parameters. Accordingly, the soil permeability depends on the effective degree of saturation S through the equation:

$$k_{rel}(S) = max\left[S_{eff}^{\ g_l}\left(1 - \left[1 - S_{eff}^{\left(\frac{g_n}{g_n - 1}\right)}\right]^{\left(\frac{g_n}{g_n-1}\right)}\right)^2 ;10^{-4}\right] \quad (2)$$

where k_{rel} denotes the relative permeability (*i.e.* the ratio between the current permeability and that of the fully-saturated soil) and g_l is a model parameter. The calibration of the Van Genuchten model (VG) was performed based on the results of controlled suction tests conducted on samples of pyroclastics (Picarelli et al., 2007) and Table 2 reports the model parameters adopted in the analyses

Table 2. *Hydraulic properties and parameters of the VG model.*

Soil	model	k_{sat} (m/s)	S_{sat}	S_{res}	g_a	g_n	g_c	g_l
Pyr. Soil	*VG*	5e-6	1	0.2	0.25	1.7	-0.38	0
Yellow Tuff	*VG*	1e-6	1	0.2	0.25	1.7	-0.38	0
Green Tuff	saturated	1e-7	-	-	-	-	-	-
Bedrock	saturated	1e-7	-	-	-	-	-	-

It should be noted that the developed numerical model was principally concerned with the geotechnical stability and seismic behaviour of the excavation slopes. It did not explicitly include the structures of the VdP, as most of these remain buried. Concerning the exposed tuff masonry walls at atrium level that are in direct contact with the right slope face, their relatively low mass was judged to have a minimal impact on the seismic response of the slope; consequently, they were omitted from the numerical model. Nevertheless, these archaeological remains will be affected by the deformation field generated by the slope's response during seismic shaking, given that the excavation face directly loads them.

Static case

The numerical analyses under static conditions, aimed at reproducing the current stress state and thus the safety conditions, were carried out according to the following phases: (1) initialization of the model's stress state through the instantaneous activation of self-weight and the generation of pore water pressu res and suction; (2) simulation of the excavation phases, proceeding in 6 steps until reaching the excavation base; (3) a steady-state seepage analysis to reproduce the pore pressure field. It is important to note that the excavation base is located at -4.5 m relative to sea level and that water present in the excavation is removed via a pumping system (e.g., De Simone, 2010). Once the effective stress field, which also accounts for the strength increase due to suction in the partially saturated soils, was determined, c'–φ' reduction analyses were performed to determine the factor of safety under static conditions and pseudo-static analyses to evaluate the critical acceleration k_c associated with the formation of a failure mechanism in the excavation front adjacent and opposite to the Villa of the Papyri. Figure 3 shows the critical mechanisms in terms of incremental deviatoric strains obtained under static conditions (Figure 3a) and those under pseudo-static conditions (Figure 3b,c). The results highlight that the excavation front adjoining the Villa of the Papyri constitutes the most critical portion, as it exhibits a factor of safety close to unity (F_s = 1.06) and a relatively low critical acceleration (k_c = 0.05g).

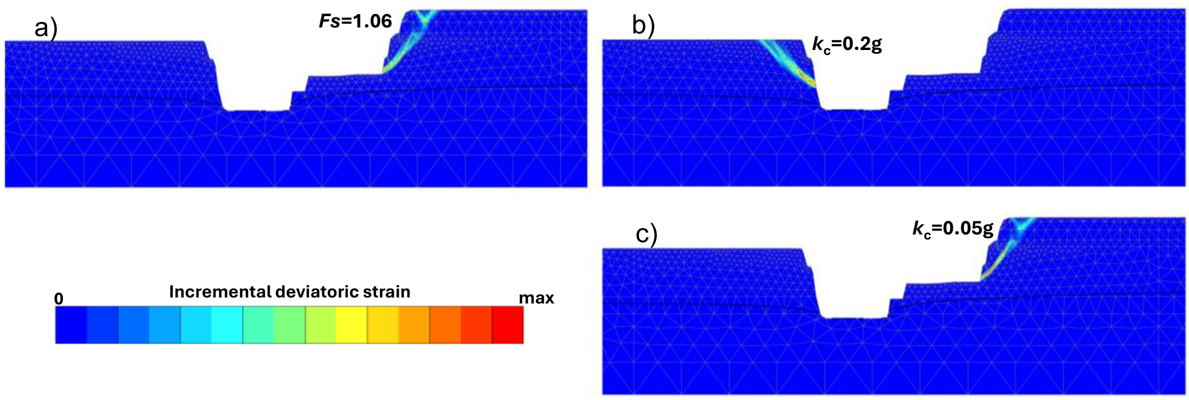

Figure 3. *Failure mechanisms: a) static conditions; b, c) pseudo-static conditions.*

Seismic case

Once the initial stress state had been reproduced, and consequently the distribution of stiffness and mobilized strength under current conditions, dynamic analyses were carried out to assess the seismic performance of the excavation fronts. These analyses were performed by applying horizontal acceleration time histories at the base of the model. These accelerograms were selected based on the requirement of compatibility with the design response spectrum specified by the Italian Technical Standards for Construction (NTC 2018) for the Life Safety Limit State, corresponding to a return period of 712 years and a peak ground acceleration (PGA) of 1.85 m/s², relative to a site on outcropping rock located in the territory of Herculaneum. The selection of input seismic motions, aimed at obtaining an average spectrum compatible with the regulatory one, was performed using the software REXELweb (Sgobba et al., 2021) based on the parameters of moment magnitude (Mw) and epicentral distance (R), extracting the signals from the Engineering Strong Motion Database (Luzi et al., 2020). The range for these parameters was set at Mw = 5.0 – 6.5 and R = 0 – 20 km, in agreement with the results of the probabilistic seismic hazard analysis developed by Stucchi et al. (2011). Compatibility with the regulatory spectrum was ensured by considering a lower tolerance of 10% and an upper tolerance of 30% within the period interval between 0.1 s and 1.5 s. The table in Figure 4 reports the earthquake metadata and the synthetic parameters of the input seismic motions returned by REXELweb based on the specified search criteria. Figure 4 shows the 5% damped elastic response spectra of the selected signals, along with their mean spectrum and the reference regulatory spectrum. Fourteen non-linear dynamic analyses were carried out, considering for each seismic input both directions of horizontal action (positive to the right). The analyses were conducted under drained conditions, thus neglecting the possible generation of seismic-induced pore water overpressures. This assumption is consistent with the results of a preliminary coupled hydro-mechanical analysis performed according to the u–p formulation (Zienkiewicz

& Shiomi, 1984). For the sake of brevity, only some representative results are reported, specifically related to the application of the first (#1) and last seismic input (#7).

Figure 5 shows the deformed mesh configuration at the end of the application of input #1 (positive direction) (Figure 5a) and input #7 (negative direction) (Figure 5b), with an amplification factor of 50. It is evident that the displacement distribution is strongly asymmetric, with the maximum displacements concentrated in the excavation front adjacent to the Villa of the Papyri. The maximum horizontal displacement values are approximately 28 mm for input #1 and 60 mm for input #7.

By comparing the deformed configuration (Figure 5) and the pseudo-static failure mechanism shown in Figure 3c, it can be observed that the deformation mechanisms highlighted in Figures 5a and 5b primarily result from the transient activation of plastic mechanisms, following the complete mobilization of shear strength during seismic loading. The triggering and extent of these mechanisms are strongly influenced by the energy content of the input signal, expressed through the Arias Intensity parameter (*Ia*), while the potential interaction between the signal's frequency content and the system's fundamental frequency plays a secondary role. Confirming this, input #1 has a predominant frequency (f_p) close to the system's fundamental frequency, whereas input #7 is characterized by a different predominant frequency and a significantly higher *Ia*.

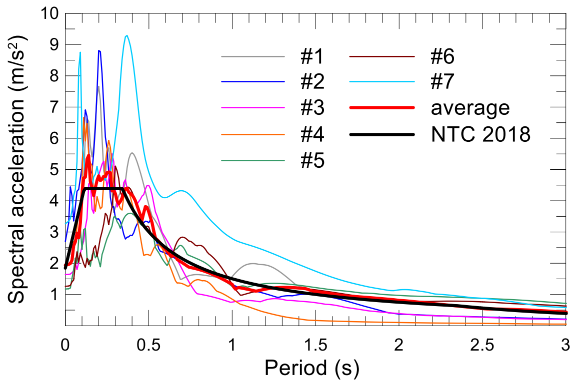

	Event name	Station	Mw	Comp.	pga (m/s^2)	Ia (m/s)	f_p (Hz)
#1	IT-1976-0030	SRC0	6.0	E	2.44	0.25	5.2
#2	EMSC-20181226_0000	SVN	5.0	N	2.77	0.28	4.2
#3	EMSC-20181226_0000	EVRN	5.0	N	1.63	0.21	1.9
#4	EMSC-20161026_0000	FEMA	5.5	E	1.93	0.23	3.9
#5	IS-2000-0053	101	6.5	3	1.17	0.18	2.1
#6	IS-2000-0053	112	6.5	2	1.26	0.22	3.2
#7	IS-2008-0054	112	6.3	3	3.27	0.52	2.6

Figure 4. *5% damped elastic response spectra of the selected signals.*

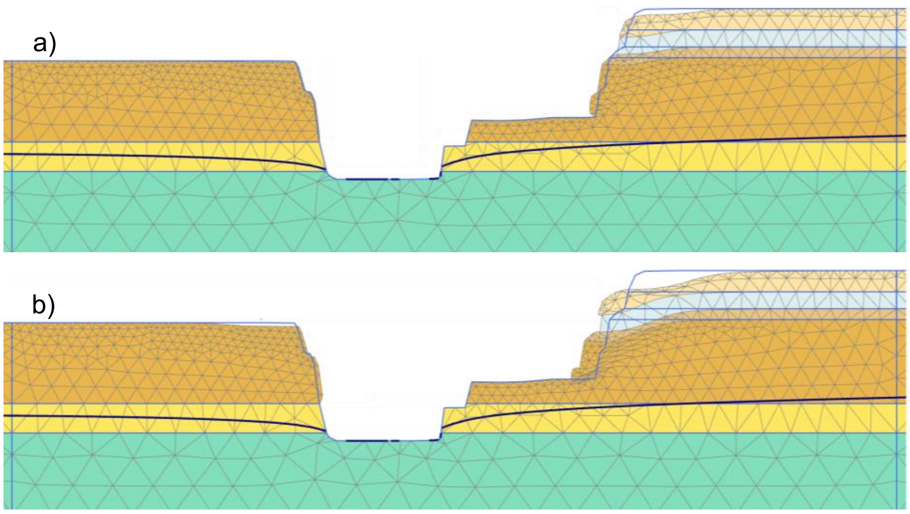

Figure 5. *Deformed mesh (amplified 50 times): a) input #1 (positive direction) and b) input #7 (negative direction).*

PERFORMANCE ASSESMENT

For the assessment of the seismic performance of the slopes, it is necessary to evaluate the admissibility of these displacement amplitudes in relation to the archaeological structures and ruins present in the study area. In this context, the seismic performance of the slopes is governed by the presence of the exposed VdP structures, represented by masonry tuff walls, which are in direct contact with the right excavation front. Consequently, the seismic performance of the right slope is dictated by the damage level that these historical masonry walls can sustain, demanding that permanent slope displacements are kept within a threshold corresponding to an acceptable damage state. A displacement-based methodology, which defines limit states for varying damage levels, offers a suitable framework for predicting the seismic performance of historical masonry walls under in-plane and out-of-plane loading. Standards such as Eurocode 8 (2005) establish this approach through three primary limit states: (i) Damage Limitation (DL), (ii) Significant Damage (SD), and (iii) Near Collapse (NC). While precise drift limits can differ, the fundamental definitions of these damage levels are aligned between Eurocode 8 (2005) and the Italian NTC (2008, 2018). Within this framework, the horizontal displacement near the slope toe—corresponding to the mid-height of the adjacent VdP masonry wall (see sketch in Figure 6)—is adopted as a performance index, providing a direct measure of both the seismic response of the slope and the damage level of the adjacent wall. The codes prescribe threshold values in terms of top drift. For the wall's expected rocking mechanism, this code-specified top drift was converted to an equivalent mid-height drift limit as a function of L, where L = h/2 = 2.5 m and h is the total wall height. Accordingly, the performance index for the excavation fronts is represented by the mid-height drift of the adjacent VDP masonry wall. Figure 6 shows a comparison between the performance index Δ evaluated for all the seismic ground motions considered plotted against the pga_{inp}; the plot the threshold values defined for each limit state provided by the relation reported in Table 3 are also shown. The comparison between Δ and these threshold fields shows that in all the cases examined the Δ obtained from the analyses correspond to the SD and NC limit states, indicating that the current seismic performance of the slope presents an unacceptable risk to the integrity of the exposed VdP masonry walls, compelling the need for immediate protective measures to mitigate co-seismic slope displacements and ensure the long-term preservation of this archaeological heritage.

Table 3. *Limit state thresholds drift values for masonry wall.*

	Damage limitation *DL*	Significant Damage *SD*		Near Collapse *NC*	
	-	Flexure	Shear	Flexure	Shear
NTC (2008)	0.3% *L*	0.8% *L*	0.4% *L*	-	-
NTC (2018)	0.2% *L*	-	-	1% *L*	0.5% *L*

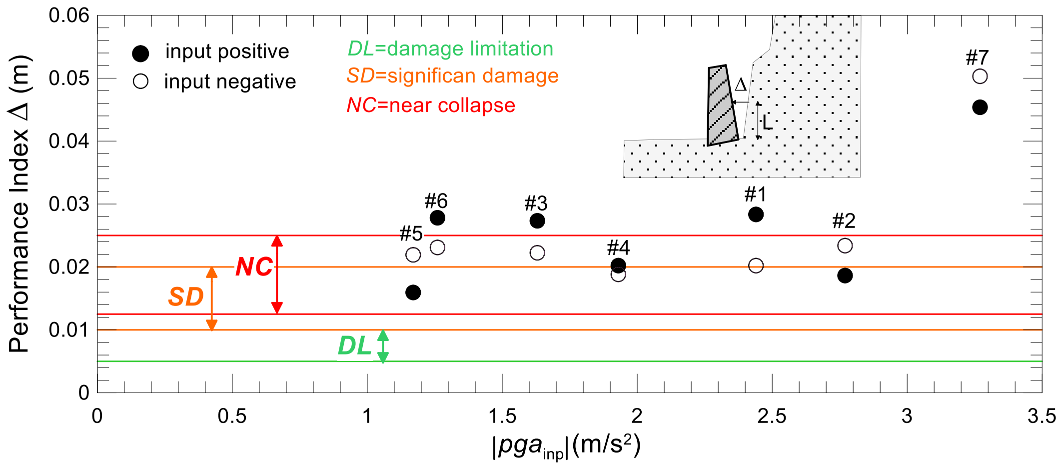

Figure 6. *Comparison between seismic performance index Δ and limit state thresholds versus pga_{inp} values of seismic ground motions.*

CONCLUSIONS

In this paper, a plane strain finite element numerical model has been developed with the aim of reproducing the current safety conditions and estimating the seismic response of the slopes near the Villa of the Papyri. This was achieved through non-linear dynamic analyses using seismic inputs compatible with the spectrum prescribed by current regulations. The results of these analyses have allowed for a preliminary assessment of the seismic performance of the excavation fronts. This assessment based on a comparison between the seismically-induced displacements and reference threshold values demonstrates that the current slope condition presents an unacceptable risk, necessitating immediate protective interventions to mitigate co-seismic displacements and ensure the long-term preservation of this archaeological heritage.

ACKNOWLEDGEMENTS

This work is part of the research activities carried out by the Research Group of the Pegaso University in the framework of the work package WP16-Slope Stability of a Research Project funded by the ReLuis (Network of Seismic Engineering University Laboratories) consortium (DPC/ReLUIS 2024-2026) and the Research Project SustaiNable preservatiOn and safety fruition of archeOlogical and cultural Sites (NOOS) - PRA 2025.

REFERENCES

Bentley, 2021. PLAXIS Connect Edition v21: A Finite Element Program for Geotechnical Engineering Problems. Bentley Systems, Delft, The Netherlands.

Borja, R.I., White, J.A., Liu, X., Wu, W., 2012. Factor of safety in a partially saturated slope inferred from hydro-mechanical continuum modeling. Int. J. Numer. Anal. Methods Geomech. 36 (2), 236–248.

De Simone A. (2010). Rediscovering the Villa of the Papyri. In The Villa of the Papyri at Herculaneum, Mantha Zarmakoupi Ed.

Eurocode 8 (2005). Design of structures for earthquake resistancepart 3: Assessment and retrofitting of buildings.

Luzi L., Lanzano G., Felicetta C., D'Amico M. C., Russo E., Sgobba S., Pacor, F., ORFEUS Working Group 5, 2020. Engineering Strong Motion Database (ESM) (Version 2.0). INGV. https://doi.org/10.13127/ESM.2

NTC, 2008. Italian Code for Structural Design (Norme tecniche per le costruzioni - NTC). D.M. 14/01/2008, Official Bullettin no. 29 of February 4th, 2008, In Italian.

NTC 2018 - DM 17/1/2018, 2018. Norme tecniche per le Costruzioni – Gazz. Uff. della Rep. Italiana, n. 42.

Picarelli L, Evangelista A, Rolandi G, Paone A, Nicotera MV, Olivares L., Scotto di Santolo A, Lampitiello S, Rolandi M (2007). Mechanical properties of pyroclastic soils in Campania Region. Proceed. Int. Symp. "Characterisation and Engineering Properties of Natural Soil", Tan TS, Phoon KK, Hight DW and Leroueil S eds., Singapore 4:2331–2384

Rippa F. (1996) -A description of pyroclastic soils that buried Pompei and Herculaneum in a.d. 79. Proc. Of the Int. Symp. On Geotechnical Engineering far the Preservation of Historic Sites, pp. 261-270.

Schanz T., Vermeer P.A., Bonnie P.G. (1999) – Hysteretic damping in a small-strain stiffness model. Proc. of the 10th Int. Symp. on Numerical Models in Geomechanics, NUMOG 10, London, pp. 737-742.

Scotto di Santolo, A., Nicotera, M. V., Ramondini, M., 2000. Analysis of instability phenomena affecting a cut slope in unsaturated pyroclastic soils. In: Landslides: in research, theory and practice (pp. 1353-1360). Thomas Telford

Sgobba, S., Felicetta, C., Russo, E., D'Amico, M., Lanzano, G., Pacor F., Luzi, L., Baraschino, R., Baltzopoulos, G., Iervolino, I., 2021. The online graphical user interface of REXELweb for the selection of accelerograms from the Engineering Strong Motion database (ESM). In: 39° Convegno GNGTS.

Stucchi, M., Meletti, C., Montaldo, V., Crowley, H., Calvi, G.M., Boschi, E., 2011. Seismic hazard assessment (2003–2009) for the Italian building code. Bulletin of the Seism. Soc. of America, 2011; 101:1885–911

Van Genuchten, M.T., 1980. A closed form equation for predicting the hydraulic conductivity of unsaturated soils. Soil Sci. Soc. Am. J. 44 (5), 892–898.

Zienkiewicz O. C., Shiomi T. (1984) – Dynamic behaviour of saturated porous media; the generalized Biot formulation and its numerical solution. International journal for numerical and analytical methods in geomechanics, 8, n. 1, pp. 71-96.